Surv Geophys (2012) 33:275–292
DOI 10.1007/s10712-011-9158-7

Two-Dimensional Geothermal Modelling Along the Central Pontides Magmatic Arc: Implications for the Geodynamic Evolution of Northern Turkey

Nafiz Maden

Received: 13 April 2011 / Accepted: 31 October 2011 / Published online: 30 November 2011

Abstract The Pontides, which can be divided tectonically into three main segments as Eastern, Central, and Western Pontides, is one of the most complex geodynamic settings within the Alpine belt. The Central Pontides, where the Eastern and Western Pontides met and formed a tectonic knot, represent an amalgamated tectonic mosaic consisting of remnants of oceanic, continental, and island arc segments. Subduction polarity, which is responsible for the formation of the Pontides, is still under debate because of limited geological, geophysical, and geochemical data. Two-dimensional (2-D) thermal modelling studies along the Central Pontides magmatic arc (Northern Turkey), Sakarya and Kırşehir continents are investigated in order to delineate the crustal thermal structure and subduction polarity. The obtained numerical results indicate that arc and back-arc regions are hot because of the cooling effects of a subducting plate. Moho temperatures in the investigated region are found between 992°C in the south (back-arc) and 415°C in the north (arc). Moreover, mantle heat flow values vary from 57.2 mWm^{-2} in the south (back-arc) to 34.7 mWm^{-2} in the north (arc). It is shown from this study that the Eurasia plate had moved from north to south under the Anatolia plate along the south Black Sea coast.

Keywords Heat flow · Thermal conductivity · Spectral analysis · Central Pontides

1 Introduction

The Central Pontides, which represent a tectonic knot where the Eastern and Western Pontide units have been tectonically juxtaposed, lie between the İzmir-Ankara suture in the south and the Black Sea in the north (Fig. 1). It is made up of approximately east–west-trending zones and includes two Pontide terranes (Sakarya and İstanbul zones). From north to the south, the Central Pontides consist of the following main components; (1) the northern zone (the magmatic belt), (2) the Kastamonu Boyabat basin fill, (3) the Araç-Daday shear zone, (4) the Kargı massif, and (5) the ophiolite belt (Yılmaz et al. 1997;

N. Maden (✉)
Department of Geophysics, Gümüşhane University, 29100 Gümüşhane, Turkey
e-mail: nmaden@gumushane.edu.tr

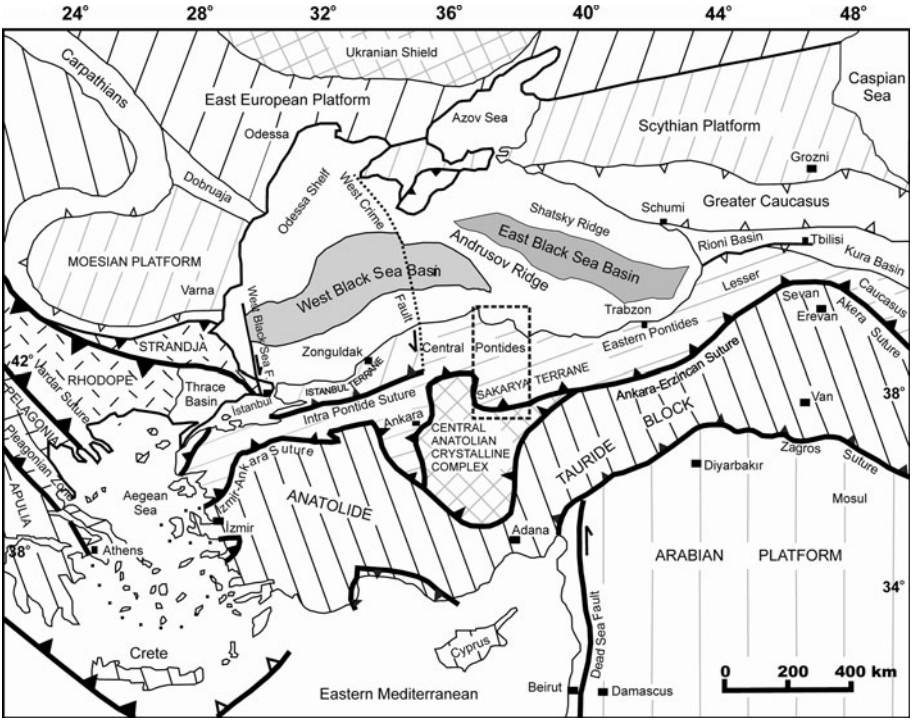

Fig. 1 Tectonic map of the Turkey and surrounding region showing the major sutures and continental blocks (Okay and Tüysüz 1999; Okay et al. 2006). The *dashed-line box* shows the location of the study area shown in Fig. 2

Okay et al. 2006) (Fig. 2). The northern zone is interpreted as an Andean type magmatic belt that developed above the passive continental margin succession during the Late Cretaceous. The Kastamonu-Boyabat basin fill was deposited within a fore arc basin formed in association with the volcanic belt. The Araç-Daday shear zone is interpreted as a highly tectonised basin fill that was deposited in the easterly narrowing oceanic remains of the Paleotethys. The Kargı massif, which composed the major part of the central Pontides, is a tectonic mosaic that is composed of various accreted tectonostratigraphic units. The ophiolite belt is characterized by the disrupted ophiolite and the late Cretaceous ophiolitic mélange association (Ustaömer and Robertson 1997; Yılmaz et al. 1997).

There are different opinions of the geotectonic evolution of the Pontides and the polarity of subduction. This argument remains controversial and has not yet been exactly solved. According to Adamia et al. (1977, 1981), Ustaömer and Robertson (1995), ultramafic rocks located in the southern Pontide Arc are a remnant of the Palaeotethys Ocean. They claimed that the Pontides emplaced over the northward-subducting Palaeotethys during much of the Paleozoic to the late Eocene. However, Şengör and Yılmaz (1981) suggested that Palaeotethys had been situated north of the Pontides, and that the southward subduction took place from the Palaeozoic until the Dogger and the northward subduction happened later, from the late Cretaceous until the end of the Eocene. According to the model of Şengör and Yılmaz (1981), the Pontides were at the southern active continental margin of Eurasia, whereas the late Cretaceous arc volcanism occurred above the northward subduction of Neotethys.

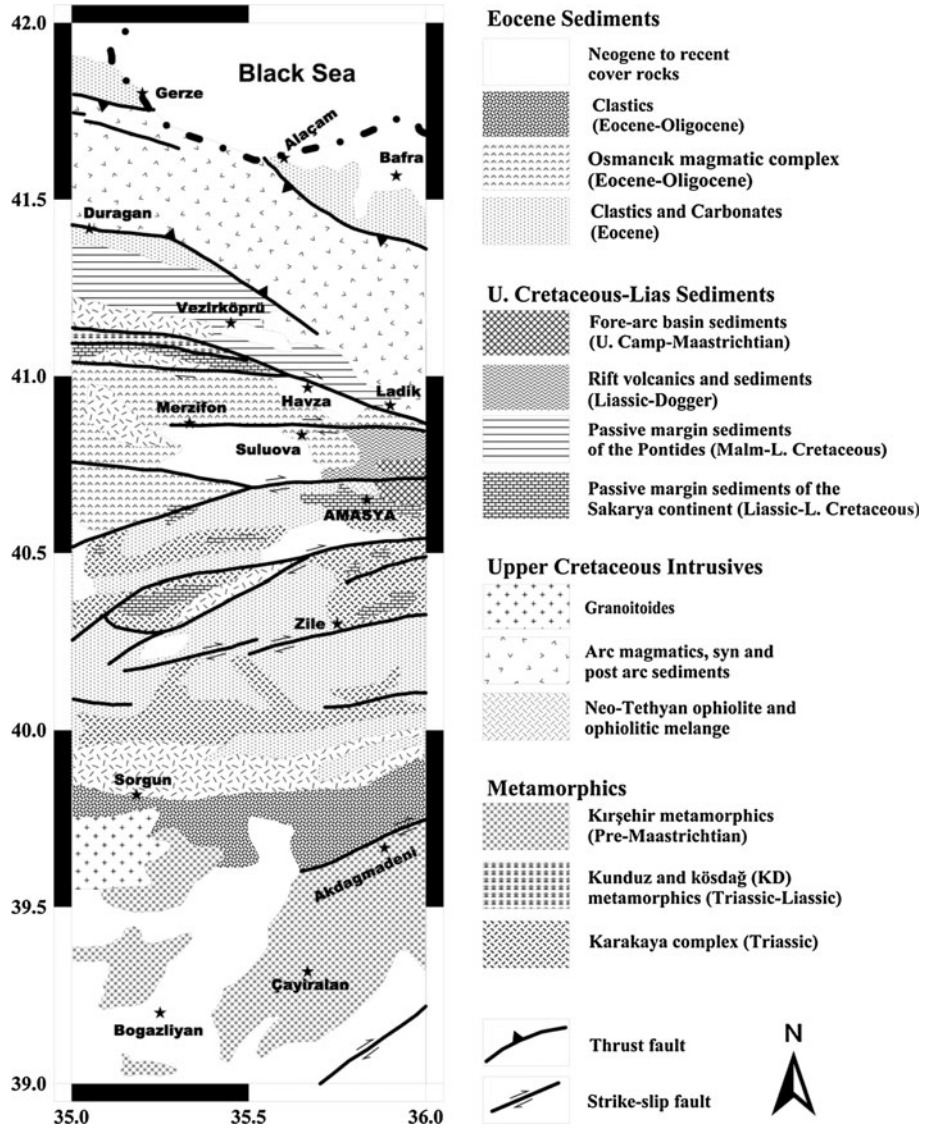

Fig. 2 Geological map of the Central Pontides (modified from Yılmaz et al. 1997)

Dewey et al. (1973), Bektaş (1986), Bektaş et al. (1984, 1987, 1999), Chorowicz et al. (1998), Eyüboğlu et al. (2006), and Eyüboğlu (2010) suggested a southward subduction model contrary to the northward subduction of Neotethys. They claimed that this southward subduction of the Paleotethys oceanic lithosphere lasted from the Paleozoic until the end of the Eocene. In this model, while the Black Sea is explained as a remnant of the Palaeotethys Ocean, the ultramafic belt exposed in the south of the arc represents portions of preserved back-arc basin.

This study is the first attempt to focus on the crustal temperatures of the Central Pontides. Most recently, based on spatial and temporal variations in the magmas generated

in the Eastern Pontide orogenic belt, Eyüboğlu et al. (2010) suggested a new geodynamic model to explain the Meso-Cenozoic tectonomagmatic evolution of the Eastern Pontide orogenic belt and correlate the adakitic magmatism to ridge subduction and slab window process within a south-dipping subduction zone.

The aim of this paper is to present numerical results of crustal temperatures and heat flows and to discuss the subduction polarity of the Central Pontides and thus try to explain the evolution of the Pontides.

2 Gravity, Curie Point Depth, and Heat Flow Data

The Bouguer anomaly data (Fig. 3) of Central Pontides, gridded at an interval of 2.5 km, were obtained from the General Directorate of Mineral Research and Exploration (MTA). Gravity values are tied to MTA and General Command of Mapping base stations related to the Potsdam absolute gravity value 981260.00 mGal accepted by the International Union of Geodesy and Geophysics in 1971. A latitude correction was applied according to the Gravity Formulae of 1967. The Bouguer reduction was done for a density of 2.40 kgm^{-3}. Topographic correction was calculated up to a distance of 167 km, assuming a terrain density of 2.67 kgm^{-3} (Maden et al. 2009a).

Gravity anomaly contour lines are parallel to magmatic belt and zero contours usually followed the Black Sea coastal line. Most of the gravity anomaly map is represented by negative anomalies. There are two strong gravity gradients located in the northern and central part of the region. The E–W-trending anomalies shown in the centre of the region correlate with İzmir-Ankara suture. The Kirsehir Block located in the south of the study area shows very large negative anomalies.

Various researchers (Ateş et al. 2005; Aydın et al. 2005; Dolmaz et al. 2005; Bektaş et al. 2007; Bilim 2007; Maden et al. 2009b; Maden 2009; Maden 2010) have carried out studies on the Curie point depth using magnetic data in Turkey. Aydın et al. (2005) made a study to prepare the Curie-point isotherm map of Turkey by using a spectral analysis technique applied to the aeromagnetic data. According to this map, the deepest Curie point depths are found in the Eastern Pontides and Western Taurus belt (20–29 km). On the other hand, the shallowest Curie point depths are found in the Central Anatolian and the Aegean region (6–10 km). Ateş et al. (2005) showed that the Curie depth values change from 7.9 to 22.6 km in Central Anatolia. Also, Dolmaz et al. (2005) estimated that the Curie point depth varies from 8.2 to 19.9 km in the Western Anatolia region. According to the Bektaş et al. (2007), the Curie point depth changes between 12.9 and 22.6 km in the Eastern Anatolia region.

Maden et al. (2009b) calculated the average Curie point depth with a spectral analysis method to be 22.2 km using magnetic data of the Eastern Pontides. They found that the Curie point depths fluctuate between 14.3 km in the south and 27.9 km in the north. Maden (2009) determined the average Curie point depth as 20.4 km, with values changing from 14.8 km in the south to 21.8 km in the north of the Central Pontides. Moreover, Maden (2010) applied a spectral analysis technique to the magnetic data of the Erciyes region and revealed that the average Curie point depth is 13.7 km, thus reflecting the high geothermal potential of the region coming from partial melting of crust.

A preliminary heat flow map of Turkey was prepared by Tezcan and Turgay (1989) with a constant thermal conductivity gathered from exploration wells. Tezcan (1995) revised this map by using temperatures measured in oil and coal wells mostly drilled in the south-eastern Turkey and Thrace basin. Additionally, İlkışık (1992) made a heat flow map of

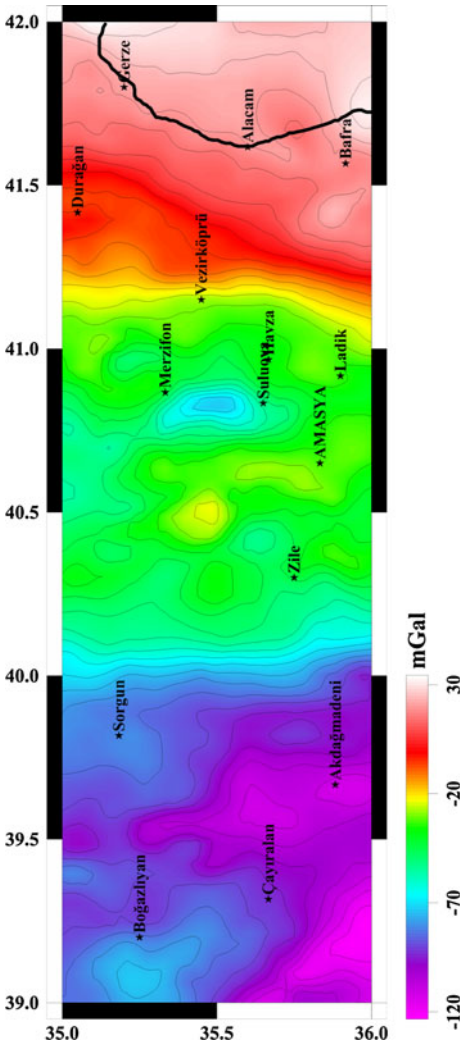

Fig. 3 Bouguer gravity map of the region; the contour interval is 5 mGal. The *colour bar* indicates interval values; *colour levels* show anomalous intensities from *magenta* (negative) to *white* (positive)

Turkey from the silica and chemical content of thermal springs. In this map, the average heat flow values were estimated in the western, the central and the eastern Anatolia to be 110.72, 102.78 and 112.81 mWm^{-2}, respectively. Later, Tezcan (1995) stated that the heat flow values for Anatolia should be much higher than those for the Mediterranean and the Black Sea.

According to the İlkışık (1995), the mean heat flow values for western Anatolia based on the silica data and the conventional heat flow data are 107 and 97 mWm^{-2}, respectively. The heat flow data of the İlkışık (1995) indicate a close relation between the high heat flow value based on silica data and Tertiary and younger volcanism. İlkışık (1995) obtained the highest heat flow value of 247 mWm^{-2} from the silica content near Gediz. In the Ihlara valley, İlkışık et al. (1997) determined the average heat flow value using both silica and gradient techniques to be 158.5 mWm^{-2}.

Recently, Maden (2009) and Maden (2010, 2011) studied the heat flow values for the Central Anatolia region and the Central Pontides. In the Central Pontides, the heat flow

values computed from the Curie depth values vary from 94.1 mWm^{-2} in the south (back arc) to 63.8 mWm^{-2} in the north (arc), showing that the south of the investigated area has relatively high geothermal potential with respect to the northern part of the region (Maden 2009). It may be possible that this phenomenon is caused by movement of the Eurasia plate under the Anatolia plate.

Maden (2010) estimated heat flow values of 88.8 and 106.5 mWm^{-2} from the silica data and conventional heat flow methods, respectively, in the Central Pontides. Maden (2011) calculated the surface heat flow values from the Curie depth values using the equation of Sharma et al. (2005). The obtained values vary between 66.5 and 104.7 mWm^{-2}. The tectonic activities after the Late Triassic as suggested by Şengör and Yılmaz (1981) and Bozkurt (2001) are related to the high heat flow values in the region.

3 Spectral Analysis Method and Crustal Structure

The spectral analysis method has been widely used to determine the depth to the top of magnetic source bodies without any prior knowledge of the geometry from the wavelengths of potential fields (Bhattacharyya 1966; Bhattacharyya and Leu 1975, 1977; Bansal and Dimri 2001; Bansal et al. 2006; Chavez et al. 1999; Curtis and Jain 1975; Gomez-Ortiz et al. 2005; Hofstetter et al. 2000; Lefort and Agarwal 2002; Nnange et al. 2000; Pal et al. 1979; Pamukcu et al. 2007; Poudjom Djomani et al. 1992; Rivero et al. 2002; Spector and Grant 1970). This method for estimating the mean depth to ensembles of magnetic sources has been generalized to gravity data (Dimitriadis et al. 1987) and can be used to map geologic structures from gravity and/or magnetic data observed at the earth's surface (Treitel et al. 1971).

In this technique, gravity data are transformed into the wave-number domain to analyse the frequency content of the information. A plot of the logarithm of the power spectrum versus frequency exhibits several straight-line segments whose slopes decrease with increasing frequency. The slopes of various segments provide an estimate of the depths to the various levels of anomalous sources. A suitable cut-off frequency separates the power spectrum curve into two domains with high and low wavelengths. The high frequency domain is associated with shallow sources, and the low frequency domain is related to deeper sources; these are called residual and regional anomalies, respectively (Spector and Grant 1970). Following Pal et al. (1979), the depth to a given ensemble of prismatic bodies, d, can be estimated from the power spectrum of the associated anomaly, by applying:

$$E(k,0) = E(0,0)e^{\left[\frac{2\pi}{N}d-m\right]k} \tag{1}$$

where k, m, and N are the wave number, the slope of the average spectrum and number of gravity data, respectively. The depth, d, to the top of the basement can be easily calculated, since the gradient of $\left[\frac{2\pi}{N}d - m\right]$ should be zero.

The gravity data were separated into five different sub-regions with dimensions of $1°\times1°$ and step intervals of 0.5° to reveal a two-dimensional (2D) Moho depth profile for the region. The gravity anomaly data of the sub-regions were transformed into the frequency domain using the 2D Fourier method. Figure 4 shows as an example the graph of the power spectra to determine the depth of the crustal interfaces for an analysis of the gravity data covering the area 35°E, 39°N to 36°E, 40°N. With the least squares method, four straight-line segments are fitted in the graph, related to different wavenumber regions. This pattern is related to the depths of different anomaly sources. The values over the linear segments are the depths to various interfaces arising from the main density contrasts within

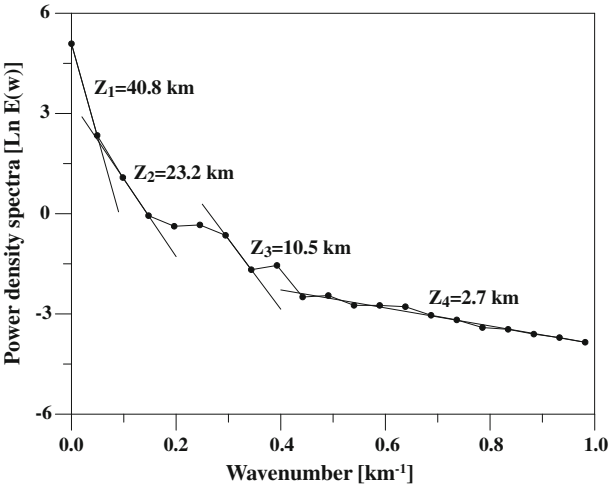

Fig. 4 Examples of power spectra curves used for determining the depth of anomaly sources computed at 39°.30′N, 35°.30′E. The values over the linear segments are the depths to various interfaces formed by crustal density contrasts. Z_1, Z_2, Z_3, and Z_4 represent the depths of the *Moho*, *lower*, *upper* crusts and the sedimentary layer, respectively, computed from the gravity values using power spectral analysis

Table 1 The depth values of the 2D crustal model of the Central Pontides computed from gravity data using the power spectrum method

Location	Sediments (km)	Upper crust (km)	Middle crust (km)	Lower crust (km)
(35.0°E, 39.0°N)–(36.0°E, 40.0°N)	2.7	10.5	23.2	40.8
(35.0°E, 39.5°N)–(36.0°E, 40.5°N)	2.5	8.9	23.1	40.1
(35.0°E, 40.0°N)–(36.0°E, 41.0°N)	2.7	11.7	20.6	36.4
(35.0°E, 40.5°N)–(36.0°E, 41.5°N)	3.1	8.2	19.4	36.2
(35.0°E, 41.0°N)–(36.0°E, 42.0°N)	2.9	10.2	17.8	27.2

the crust. Computations have been carried out for each sub-region with a window length of 1 degrees and a step interval of 0.5 degrees, separately.

The low wavenumber region between 0 and 0.09 km^{-1} representing the contribution of the long wavelength sources is considered to be a result of the density difference at the Moho discontinuity (40.8 km). An intermediate wavenumber region in the interval of 0.09–0.15 km^{-1} is associated with the density difference between the middle and the lower crust called the Conrad interface (23.2 km). The wavenumber region between 0.25 and 0.35 km^{-1} gives the upper crust depth of 10.5 km. The fourth region having wavenumbers between 0.4 and 0.98 km is related to the sediment layer (depth 2.7 km).

The two-dimensional crustal structure of the study area obtained with the above determined values for the five sub-regions is listed in Table 1. The Moho depth increases from 27.1 km in the north (arc) to 40.8 km in the south (back arc) (Fig. 5). In the back arc regions, where the crust is thicker, the heat flow value is rather high (94.1 mWm^{-2}) with respect to the arc region, where the crust is thinner (63.8 mWm^{-2}) (Maden 2009).

4 Thermal Parameters

In order to calculate crustal temperatures for the region, it is necessary to fix the thermal conductivity and the radiogenic heat production values of the crustal layers. Many relations

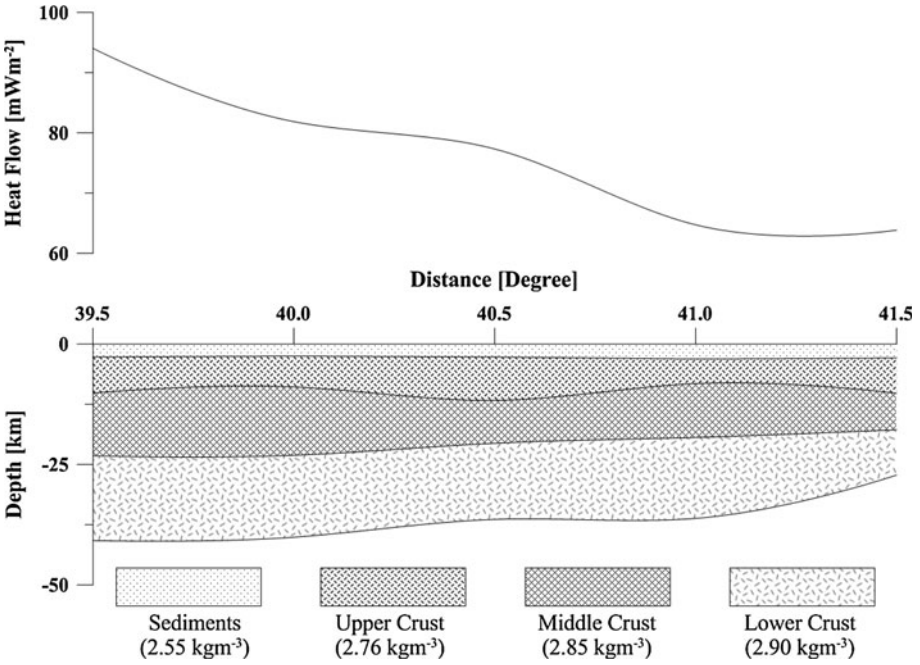

Fig. 5 Heat flow profile and 2-D crustal structure section for the Central Pontides

have been proposed which outline the variation of the thermal conductivity of different geological materials.

Throughout the crust, the thermal conductivity varies with the composition and with both the pressure and the temperature. The thermal conductivity of most crustal rocks varies inversely with temperature and tends to increase with depth (or increasing pressure) according to the following equation:

$$k = \frac{k_0(1 + bz)}{1 + cT} \tag{2}$$

where k_0 represents the thermal conductivity for surface conditions, b and c are experimental constants that control the behaviour of k depending on the lithology (Chapman and Furlong 1992).

According to some authors, the pressure effect on the thermal conductivity is negligible (Kukkonen et al. 1999; Rimi 1999: Mall and Sharma 2009), and the thermal conductivity is temperature dependent with the following relation:

$$k = \frac{k_0}{1 + cT} \tag{3}$$

where k_0 is the thermal conductivity measured at one atmosphere pressure and at 0°C; c is a material constant (Cermak and Bodri 1986). In this study, the thermal conductivity is assumed to be temperature dependent as suggested by Cermak and Bodri (1986). Jokinen and Kukkonen (1999a, b) have given thermal conductivity values for the upper, the middle, the lower crust and the mantle as 3.5, 3.0, 2.5, and 4.0 $Wm^{-1}K^{-1}$. He et al. (2009) suggested the use of thermal conductivity values of 2.9, 2.8, 2.5, and 3.0 $Wm^{-1}K^{-1}$for the

Table 2 Thermal conductivity and heat production values used for the geotherm calculation

Layer	Thermal conductivity (Wm^{-1} $K^{-1)}$)	Heat production (μWm^{-3})
Sediments	3.14[1]	2.20[2]
Upper crust	3.5[3]	1.80[3]
Middle crust	3.0[3]	0.83[4]
Lower crust	2.5[3]	0.37[4]
Lithospheric mantle	4.0[3]	0.002[3]

References: [1] Rao et al. (1970), [2] Rimi (1999), [3] Jokinen and Kukkonen (1999a), [4] He et al. 2009

upper, the middle, the lower crust, and the upper mantle, respectively. Correia and Ramalho (1999) used the thermal conductivity values for the upper, the middle and the lower crust as 2.7, 2.5, and 2.1 $Wm^{-1}K^{-1}$, respectively, as suggested by Correia and Jones (1995). The value of 3.14 $Wm^{-1}K^{-1}$ has been used as the thermal conductivity for the sediments (Rao et al. 1970). Turcotte and Schubert (2002) suggested that the thermal conductivity of the basalts and the granites is 1.3–2.9 and 2.4–3.8 $Wm^{-1}K^{-1}$, respectively. The thermal conductivity values used in this study are listed in Table 2 and shown in Fig. 6.

Heat production values depend on the lithological and geochemical characteristics of the rock formations. While depleted mantle shows low heat production values, upper crustal rocks have high heat production values (Moisio and Kaikkonen 2006). The values of the radiogenic heat production for the upper crustal metamorphic rocks range between 1.5 and 3.5 μWm^{-3}. However, most of the values lie between 2 and 3 μWm^{-3} (Förster and Förster 2000). Rimi (1999) suggested the heat production values for the sediments as 2.20 μWm^{-3}. He et al. (2009) used heat production values for the upper, the middle, and the lower crusts of 1.10, 0.83, 0.37, and 0.24 μWm^{-3}, respectively. In addition, Jokinen and Kukkonen (1999a) used heat production values for the upper, the middle, and the lower crust and the lithospeheric mantle as 1.8, 0.6, 0.2, and 0.002 μWm^{-3}, respectively. The heat production values used in this computation for the sedimentary layer, the upper, the middle, the lower crusts and the lithospheric mantle are listed in Table 2 and shown in Fig. 6.

A number of models suggested that the radiogenic heat production is related to processes of magmatic differentiation within the crust, and several laws were invoked to

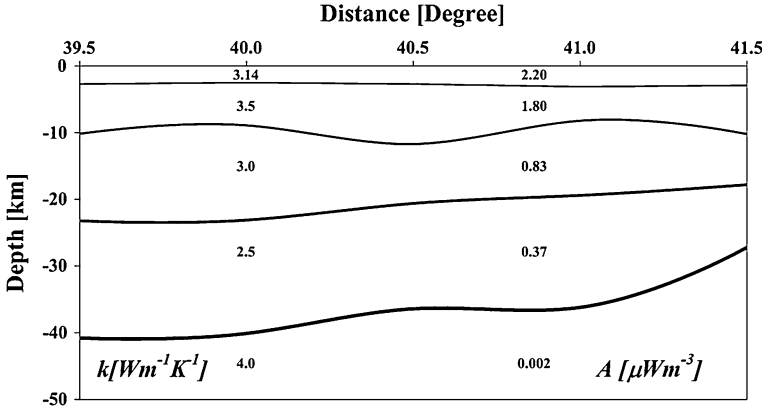

Fig. 6 Thermal conductivity (k) and heat production rate (A) of the 2-dimensional thermal model along the Central Pontides

describe the decrease with depth (Cermak et al. 1991). The most accepted model is the exponential model defined by Lachenbruch (1970),

$$A(z) = A_o e^{-\frac{z}{D}} \tag{4}$$

where A_0 is the surface heat production in μWm^{-3} and D represents the thickness of the crustal layer in km which is radioactively enriched. Factor D is derived from the surface and the reduced heat flow and generally ranges from 5 km to 15 km with an average of 10 km (Morgan and Sass 1984; Pasquale 1987).

Heat production within the crust due to the decay of the radioactive elements (U, Th, K) is the main source that contributes to the surface heat flow density (Rai and Thiagarajan 2006). Crustal radioactivity in the uppermost 10 km is affected by tectonics, metamorphism, magmatic intrusion, or U and Th redistribution processes by the presence of micro-cracks and fluid circulation. In the uppermost 10 km, groundwater movement through micro-crack systems may cause an enrichment of radioactive elements in the near surface rocks (Cermak and Rybach 1989). The distribution of the radiogenic heat-producing materials in the continental lithosphere provides an important constraint on the crustal evolution, the depletion of the mantle and the thermal evolution of the earth (Perry et al. 2006; Kumar et al. 2007).

For the study region, the heat production versus depth graphs for the five sub-regions are seen in Fig. 7. In the graphs, a sharp decrease is seen in the differentiation rate of the crustal radioactivity. The thickness of the radioactively enriched crustal layer (Table 3) varies from 12.87 km in the south to 9.82 km in the north.

5 2-D Geothermal Modelling

The presentation of the temperature variation with depth is called a geotherm. For the stable or steady state case, which means there is no change of the temperature with time, the heat conduction equation (Stüwe 2007) is given by

$$\frac{\partial^2 T}{\partial z^2} = -\frac{A_0}{k} \tag{5}$$

where T is the temperature (°C), A_0 is the radioactive heat production in μWm^{-3}, k is the thermal conductivity in $Wm^{-1}K^{-1}$, and z is the depth in m. The integration of this partial differential equation forms the basis for all calculations of stable geotherms. In the case of constant heat production, the analytical solution to the heat equation can be given by the following equation of Cermak et al. (1991),

$$T(z) = T_0 + \frac{Q_s}{k} z - \frac{A_0}{2k} z^2 \tag{6}$$

where T is the temperature at depth z in °C, T_0 is the temperature at the earth's surface, Q_s is the surface heat flow values in mWm^{-2}, k is the thermal conductivity in $Wm^{-1}K^{-1}$, and A_0 is the surface heat production value in μWm^{-3}.

Birch et al. (1968) proposed a linear relationship between the surface heat flow values and the heat production, as

$$Q_s = q_r + DA_0 \tag{7}$$

where A_0 is the surface heat production in μWm^{-3}, Q_s and q_r represent the surface and the reduced heat flow values in mWm^{-2}. The slope D characterizes the heat source

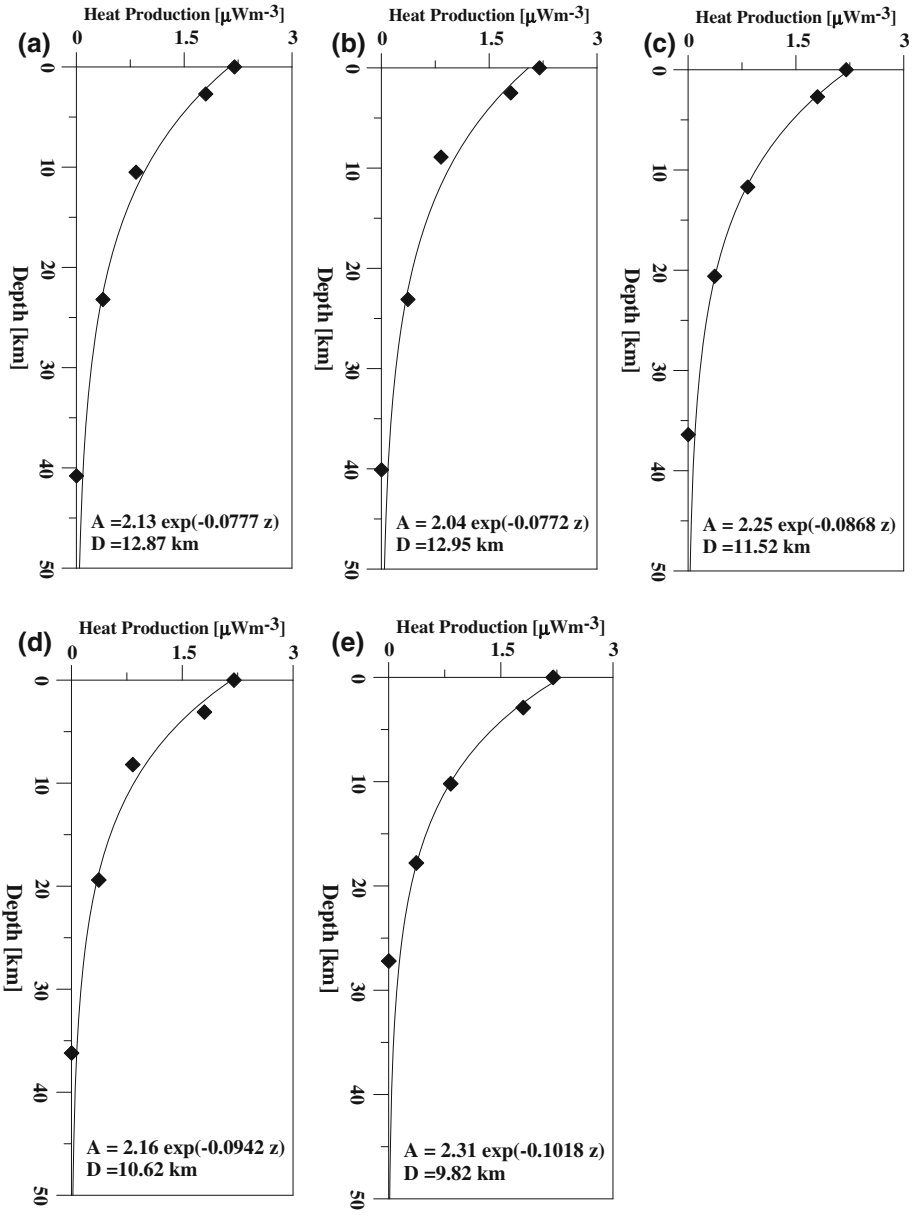

Fig. 7 Heat production versus depth graphs for the 39.5 (**a**), 40 (**b**), 40.5 (**c**), 41 (**d**), and 41.5 (**e**) degree latitude along the Central Pontide Orogenic belt. The *values* of the crustal thickness are obtained from the power spectral analysis

distribution in the upper crust. Pollack and Chapman (1977) empirically established that 60% of the surface heat flow density is attributed to the mantle heat flow, whereas 40% is generated by the radiogenic sources of the upper crust.

Table 3 Numerical results obtained from the geotherm calculations using the constant heat production model

Location	Radioactive enriched crust (km)	Moho temperature (°C)	Moho heat flow (mWm^{-2})	Reduced heat flow (mWm^{-2})
(35.0°E, 39.0°N)–(36.0°E, 40.0°N)	12.87	992	57.2	66.7
(35.0°E, 39.5°N)–(36.0°E, 40.5°N)	12.95	817	46.8	55.5
(35.0°E, 40.0°N)–(36.0°E, 41.0°N)	11.52	738	40.9	51.4
(35.0°E, 40.5°N)–(36.0°E, 41.5°N)	10.62	565	33.3	41.8
(35.0°E, 41.0°N)–(36.0°E, 42.0°N)	9.82	415	34.7	41.2

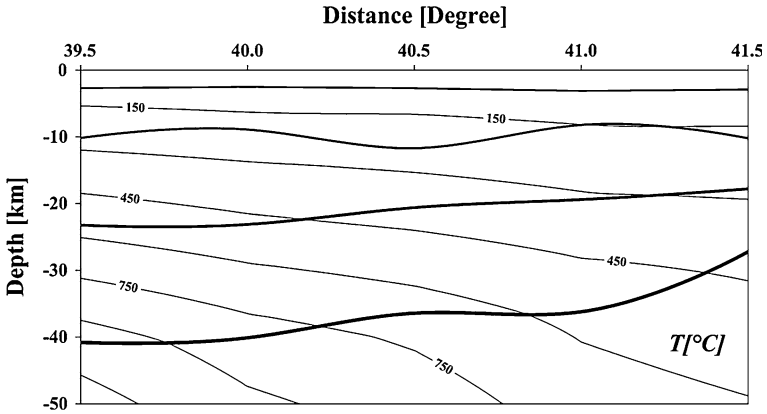

Fig. 8 The two-dimensional north–south cross section of sub-surface temperature for the Central Pontides. *Thin lines* show the temperature contours, and *thick lines* show the crustal layers

6 Discussion

In this study, a two-dimensional thermal model is derived for the Central Pontides Orogenic Belt and surrounding regions for understanding and discussing the evolution of the Pontides and subduction polarity. First, a two-dimensional crustal structure was constructed from the gravity data with a spectral analysis method. According to this model, the depth of the Moho is 27.2 km in the north (arc) and 40.8 km in the south (back arc).

The numerical results of the geotherm calculation reveal that the Moho temperature (Table 3, Fig. 8) varies from 992°C in the back arc region, where the crust is thick, to 415°C in the arc region, where the crust is thin. The surface heat flow values estimated from the Curie depth values change from 94.1 mWm^{-2} in the south (back arc) to 63.8 mWm^{-2} in the north (arc) which shows that the arc region has relatively low geothermal potential compared with the back arc region (Maden 2009). High heat flow values might be related to melting of the lithospheric mantle caused by upwelling of the asthenosphere.

The mantle heat flow values (Table 3, Fig. 9) change from 57.2 mWm^{-2} in the south (back arc) to 34.7 mWm^{-2}in the north (arc). The reduced heat flow values obtained from the exponential heat production model defined by Lachenbruch (1970) are found between 66.7 mWm^{-2} in the south (back arc) and 41.2 mWm^{-2} in the north (arc) using

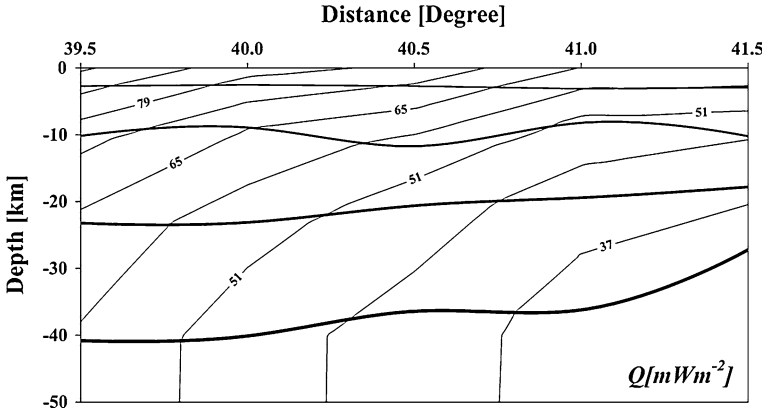

Fig. 9 2-D cross section of the heat flow values for the region calculated in this study. *Thin lines* show the heat flow contours, and *thick lines* show the crustal layers

equation (7). The graph of the reduced heat flow versus surface heat flow values indicates that they are proportional, with a linear relationship

$$Q_s = 1.2q_r + 15.2 \tag{8}$$

(see Fig. 10). In this graph, the large correlation coefficient (0.99) shows that the reliability of the results is rather high. The results obtained support the southward subduction of the Tethys oceanic plate, which is situated between Eurasia and Pontides, below the Pontide plate along the south Black sea coast (Fig. 11).

On the other hand, the Curie point surface determined from Maden (2009) in this region changes from 14.8 km in the back arc to 21.8 km in the arc, showing the cooling effect of the subducting plate and clarifying the southerly dipping opinion which was previously proposed by Dewey et al. (1973), Bektaş (1986), Bektaş et al. (1984, 1987, 1999), Chorowicz et al. (1998), Eyüboğlu (2010), and Eyüboğlu et al. (2010).

The paleomagnetic data suggest that the Pontides was located at 23° (Van der Voo 1968; Lauer 1981; Sarıbudak 1989), 25.5 ± 4.5° (Channell et al. 1996), 20.0 ± 2.5° (Çinku et al. 2010) and 26.6° (Hisarlı 2011) north latitude in the late Cretaceous, and

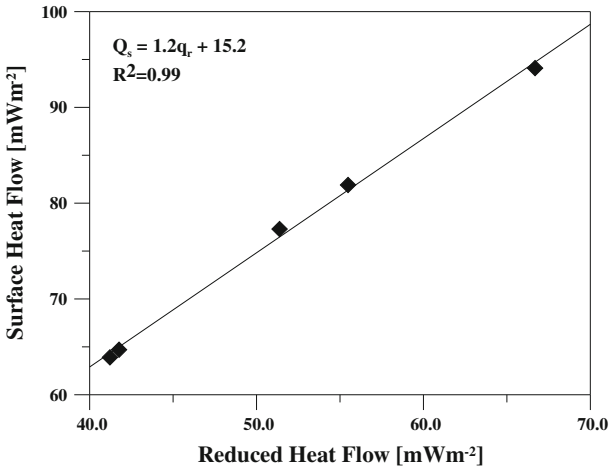

Fig. 10 Plot of the reduced heat flow versus surface heat flow data and the best fit line

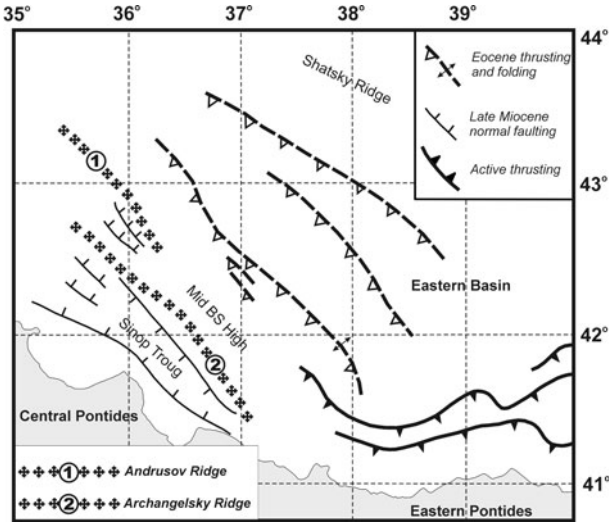

Fig. 11 Structural map based on the interpretation of the BLACKSIS profiles, illustrating the three distinct tectonic events identified in the area studied (Rangin et al. 2002)

showing that it moved to its present latitude during the Cenozoic. This northward motion of the Pontide magmatic arc supports a southward subduction model for the origin of the Pontides.

7 Conclusions

The following conclusions can be drawn from this study:

1. While the Moho thickens from north (27.2 km) to south (40.8 km), the depth to Curie point surface thickens from south (14.8 km) to north (21.8 km) along the central Pontides as stated by Maden (2009); this shows that the arc region has a relatively low geothermal potential with respect to the back-arc region.
2. The Moho temperature increases from 415°C in the arc to 992°C in the back-arc region, which may be related to the input of water into the subduction zone during southward subduction of the Tethys oceanic lithosphere below the Pontide plate along the south Black sea coast.
3. The depth of the radioactively enriched crustal layer varies from 9.82 km in the arc to 12.87 km in the back-arc region.
4. The surface heat flow value rises from 63.8 mWm^{-2} in the arc to 94.1 mWm^{-2} in the back arc region (Maden 2009).
5. The mantle heat flow values change from 34.7 mWm^{-2} in the arc to 57.2 mWm^{-2} in the back-arc regions. According to the exponential heat production model defined by Lachenbruch (1970), the reduced heat flow values vary between 66.7 mWm^{-2} in the south (back arc) and 41.2 mWm^{-2} in the north (arc).
6. The results support the southward subduction model for the origin of the Pontides during the late Mesozoic-Cenozoic.

Acknowledgments I would like to thank the General Directorate of the Mineral Research and Exploration (MTA) of Turkey for the provision of gravity data. I express my thanks to two anonymous referees for their thorough, critical and constructive comments. The author is grateful to Michael J. Rycroft for his editorial advice which improved the quality of this paper.

References

Adamia S, Lordkipanidze MB, Zakariadze GS (1977) Evolution of an active continental margin as exemplified by the Alpine history of the Caucasus. Tectonophysics 40:183–189

Adamia SA, Chkhotua T, Kekelia M, Lordkipanidze M, Shavisvili I, Zahariadze F (1981) Tectonics of the caucasus and adjoining regions: implications for the evolution of the Tethys Ocean. J Struct Geol 3:437–447

Ateş A, Bilim F, Büyüksaraç A (2005) Curie point depth investigation of Central Anatolian Turkey. Pure Appl Geophys 162:357–371

Aydın I, Karat HI, Koçak A (2005) Curie-point depth map of Turkey. Geophys J Int 162:633–640

Bansal AR, Dimri VP (2001) Depth estimation from the scaling power spectral density of nonstationary gravity profile. Pure Appl Geophys 158:799–812

Bansal AR, Dimri VP, Sagar GV (2006) Depth estimation from gravity data using the maximum entropy method (MEM) and the multi taper method (MTM). Pure Appl Geophys 163:1417–1434

Bektaş Ö (1986) Paleostress trajectories and polyphase rifting in arc-back arc of Eastern Pontides, vol 103/104. Mineral Research and Exploration Institute (MTA) Bulletin, Ankara, pp 1–15

Bektaş Ö, Van A, Boynukalın S (1987) Jurassic volcanism and its geotectonics in the eastern Pontides (NE Turkey). Geol Bull Turk 30:9–18

Bektaş Ö, Pelin S, Korkmaz S (1984) Mantle uprising and polygenetic ophiolite fact in the back-arc basin of the Eastern Pontides. In: TJK Ketin symposium, Ankara, Turkey, pp 175–188

Bektaş Ö, Şen C, Atıcı Y, Köprübaşı N (1999) Migration of the upper cretaceous subduction-related volcanism towards the back-arc basin of the Eastern Pontide magmatic arc (NE Turkey). Geol J 34:95–106

Bektaş Ö, Ravat D, Büyüksaraç A, Bilim F, Ateş A (2007) Regional geothermal characterization of East Anatolia from aeromagnetic, heat flow and gravity data. Pure Appl Geophys 164:975–998

Bhattacharyya BK (1966) Continuous spectrum of the total magnetic data due to a rectangular prismatic body. Geophysics 31:97–121

Bhattacharyya BK, Leu LK (1975) Spectral analysis of gravity and magnetic anomalies due to two-dimensional structures. Geophysics 40:993–1013

Bhattacharyya BK, Leu LK (1977) Spectral analysis of gravity and magnetic anomalies due to rectangular prismatic bodies. Geophysics 42:41–50

Bilim F (2007) Investigations into the tectonic lineaments and thermal structure of Kutahya–Denizli region, western Anatolia, from using aeromagnetic, gravity and seismological data. Phys Earth Planet Interiors 165:135–146

Birch F, Roy RF, Decker ER (1968) Heat flow and thermal history in New England and New York. In: Zen E, White WS, Hadley JB, Thompson JB Jr (eds) Studies of appalachian geology: northern and maritime. Interscience, New York, pp 437–451

Bozkurt E (2001) Neotectonics of Turkey–a synthesis. Geodinamica Acta 14:3–30

Cermak V, Bodri L (1986) Tow-dimensional temperature modeling along five east-European geotraverses. J Geodyn 5:133–163

Cermak V, Rybach L (1989) Vertical distribution of heat production in the continental crust. Tectonophysics 159:217–230

Cermak V, Bodri L, Rybach L (1991) Radioactive heat production in the continental crust and its depth dependence. In: Cermak V, Rybach L (eds) Terrestrial heat flow and the lithosphere structure. Springer, New York, pp 23–69

Channell JET, Tüysüz O, Bektaş O, Şengör AMC (1996) Jurassic-Cretaceous paleomagnetism and paleogeography of the Pontides (Turkey). Tectonics 115:201–212

Chapman DS, Furlong KP (1992) Thermal state of the continental lower crust. In: Fountain DM, Arculus R, Kay RW (eds) continental lower crust. Elsevier, Amsterdam, pp 179–198

Chavez RE, Lazaro-Mancilla O, Campos-Enriquez JO, Flores-Marquez EL (1999) Basement topography of the Mexicali valley from spectral and ideal body analysis of gravity data. J S Am Earth Sci 12: 579–587

Chorowicz J, Dhont D, Adıyaman Ö (1998) Black sea Pontide relationship: interpretation in terms of subduction. In: Third international Turkish geology symposium, Abstracts, Ankara, Turkey, METU, p 258

Çinku MC, Ustaömer T, Hirt AM, Hisarli ZM, Heller F, Orbay N (2010) Southward migration of arc magmatism during latest Cretaceous associated with slab steepening, East Pontides, N Turkey: new paleomagnetic data from the Amasya region. Phys Earth Planet Interiors 182:18–29

Correia A, Jones FW (1995) A magnetotelluric survey in a reported geothermal area in southern Portugal. Proc World Geotherm Congr 2:927–931

Correia A, Ramalho EC (1999) One-dimensional thermal models constrained by seismic velocities and surface radiogenic heat production for two main geotectonic units in southern Portugal. Tectonophysics 306:261–268

Curtis CE, Jain S (1975) Determination of volcanic thickness and underlying structures from aeromagnetic maps of the Silet area of Algeria. Geophysics 40:79–90

Dewey JF, Pitman WC, Ryan WBF, Bonin J (1973) Plate tectonics and the evolution of the Alpine system. Geol Soc Am Bull 84:3137–3180

Dimitriadis K, Tselentis GA, Thanassoulas K (1987) A basic program for 2-D spectral analysis of gravity data and source depth determination. Comput Geosci 13:549–560

Dolmaz MN, Hisarlı ZM, Ustaömer T, Orbay N (2005) Curie point depths based on spectrum analysis of aeromagnetic data, West Anatolian extensional province, Turkey. Pure ApplGeophys 162:571–590

Eyüboğlu Y (2010) Late cretaceous high-K volcanism in the eastern pontide orogenic belt: implications for the geodynamic evolution of NE Turkey. Int Geol Rev 52:142–186

Eyüboğlu Y, Bektaş O, Şeren A, Maden N, Özer R, Jacoby WR (2006) Three-directional extensional deformation and formation of the liassic rift basins in the Eastern Pontides (NE Turkey). Geol Carpathica 57:337–346

Eyüboğlu Y, Chung SL, Santosh M, Dudas FO, Akaryali E (2010) Transition from shoshonitic to adakitic magmatism in the Eastern Pontides, NE Turkey: implications for slab window melting. Gondwana Res 19:413–429

Förster A, Förster HJ (2000) Crustal composition and mantle heat flow: implications from surface heat flow and radiogenic heat production in the Variscan Erzgebirge (Germany). J Geophys Res 105(B12): 27.917–27.938

Gomez-Ortiz D, Tejero-Lopez R, Babin-Vich R, Rivas-Ponce A (2005) Crustal density structure in the Spanish central system derived from gravity data analysis (Central Spain). Tectonophysics 403: 131–149

He L, Hu S, Yang W, Wang J (2009) Radiogenic heat production in the lithosphere of Sulu ultrahigh-pressure metamorphic belt. Earth Planet Sci Lett 277:525–538

Hisarlı ZM (2011) New paleomagnetic constraints on the late cretaceous and early Cenozoic tectonic history of the Eastern Pontides. J Geodyn. doi:10.1016/j.jog.2010.12.004

Hofstetter A, Dorbath C, Rybakov M, Goldshmidt V (2000) Crustal and upper mantle structure across the Dead Sea rift and Israel from teleseismic P-wave tomography and gravity data. Tectonophysics 327:37–59

İlkışık OM (1992) Silica heat flow estimates and lithospheric temperature in Anatolia. In: Proceedings, XI. congress of world hydrothermal organization, İstanbul, Mayıs, pp 92–104

İlkışık OM (1995) Regional heat flow in western Anatolia using silica temperature estimates from thermal springs. Tectonophysics 244:175–184

İlkışık OM, Gürer A, Tokgöz T, Kaya C (1997) Geoelectromagnetic and geothermic investigations in Ihlara Valley Geothermal Field. J Volcanol Geotherm Res 78:297–308

Jokinen J, Kukkonen IT (1999a) Random modelling of the lithospheric thermal regime: forward simulations applied to uncertainty analysis. Tectonophysics 306:277–292

Jokinen J, Kukkonen IT (1999b) Inverse simulation of the lithospheric thermal regime using the Monte Carlo method. Tectonophysics 306:293–310

Kukkonen IT, Jokinen J, Seipold U (1999) Temperature and pressure dependencies of thermal transport properties of rocks: implications for uncertainties in thermal lithosphere models and new laboratory measurements of high-grade rocks in the central Fennoscandian shield. Surv Geophys 20:33–59

Kumar PS, Menon R, Reddy GK (2007) The role of radiogenic heat production in the thermal evolution of a Proterozoic granulite-facies orogenic belt: Eastern Ghats, Indian Shield. Earth Planet Sci Lett 254: 39–54

Lachenbruch AH (1970) Crustal temperature and heat production: implication of the linear heat flow relationship. J Geophys Res 75:3291–3300

Lauer JP (1981) Orgine meridionale des Pontides d'apres de nouevaux resultats paleomagnetiques obtenus en Turqie. Bulletin de la Societe Geologique de France 23:619–624

Lefort JP, Agarwal BNP (2002) Topography of the Moho undulations in France from gravity data: their age and origin. Tectonophysics 350:193–213
Maden N (2009) Crustal thermal properties deduced from spectral analysis of magnetic data in Central Pontides (Turkey). Turk J Earth Sci 18:383–392
Maden N (2010) Curie-point depth from spectral analysis of magnetic data in Erciyes stratovolcano (Central TURKEY). Pure Appl Geophys 167:349–358
Maden N (2011) One dimensional thermal modeling of the Eastern Pontide Orogenic Belt (NE TURKEY). Pure Appl Geophys. doi:10.1007/s00024-011-0296-0
Maden N, Gelişli K, Bektaş O, Eyüboğlu Y (2009a) Two-and-three-dimensional crust topography of the Eastern Pontides (NE TURKEY). Turk J Earth Sci 18:225–238
Maden N, Gelişli K, Eyüboğlu Y, Bektaş O (2009b) Determination of tectonic and crustal structure of the Eastern Pontide Orogenic Belt (NE Turkey). Pure Appl Geophys 166:1987–2006
Mall DM, Sharma SR (2009) Tectonics and thermal structure of western Satpura, India. J Asian Earth Sci 34:450–457
Moisio K, Kaikkonen P (2006) Three-dimensional numerical thermal and rheological modelling in the central Fennoscandian Shield. J Geodyn 42:95–114
Morgan P, Sass JH (1984) Thermal regime of the continental lithosphere. J Geodyn 1:143–166
Nnange JM, Ngako V, Fairhead JD, Ebinger CJ (2000) Depths to density discontinuities beneath the Adamawa plateau region, Central Africa, from spectral analyses of new and existing gravity data. J Afr Earth Sc 30:887–901
Okay AI, Tüysüz O (1999) Tethyan sutures of northern Turkey. In: Durand B, Jolivet L, Horváth F, Séranne M (eds) The mediterranean basins: tertiary extension within the Alpine orogen, vol 156. Geological Society of London, Special Publication, London, pp 475–515
Okay AI, Tüysüz O, Satır M, Altıner SÖ, Altıner D, Sherlock S, Eren RH (2006) Cretaceous and Triassic subduction-accretion, HP/LT metamorphism and continental growth in the central Pontides, Turkey. Geol Soc Am Bull 118:1247–1269
Pal PC, Khurana KK, Unnikrishna P (1979) Two examples of spectral approach to source depth determination in gravity and magnetics. Pure Appl Geophys 117:772–783
Pamukcu OA, Akcig Z, Demirbas S, Zor E (2007) Investigation of crustal thickness in Eastern Anatolia using gravity, magnetic and topographic data. Pure Appl Geophys 164:2345–2358
Pasquale V (1987) Possible thermal structure of the eastern part of the Central Alps. Nuovo Cimento 10C:129–141
Perry FV, Valentine GA, Cogbill AH, Keating GN, Gaffney ES, Damjanac B (2006) Control of basaltic feeder dike orientation by fault capture near Yucca Mountain, USA, American Geophysical Union Fall Meeting, San Francisco, abstract V11B-0572
Pollack HN, Chapman DS (1977) On the regional variation of heat flow, geotherms and lithosphere thickness. Tectonophysics 38:279–396
Poudjom Djomani YH, Diament M, Albouy Y (1992) Mechanical behaviour of the lithosphere beneath the Adamawa Uplift (Cameroon, West Africa) based on gravity data. J Afr Earth Sc 15:81–90
Rai SN, Thiagarajan S (2006) A tentative 2D thermal model of central India across the Narmada-Son Lineament (NSL). J Asian Earth Sci 28:363–371
Rangin C, Bader AG, Pascal G, Ecevitoğlu B, Görür N (2002) Deep structure of the Mid Black Sea High (offshore Turkey) imaged by multi-channel seismic survey (BLACKSIS cruise). Mar Geol 182:265–278
Rao RUM, Verma RK, Gupta ML (1970) Heat flow at Dam and Mohapani, Satpura Gondwana basin India. Earth Planet Sci Lett 7:406–412
Rimi A (1999) Mantle heat flow and geotherms for the main geologic domains in Morocco. Int J Earth Sci 88:458–466
Rivero L, Pinto V, Casas A (2002) Moho depth structure of the eastern part of the Pyrenean belt derived from gravity data. J Geodyn 33:315–332
Sarıbudak M (1989) New results and a paleomagnetic overview of the Pontides in Northern Turkey. Geophys J Int 99:521–531
Şengör AMC, Yılmaz Y (1981) Tethyan evolution of Turkey: a plate tectonic approach. Tectonophysics 75:181–241
Sharma SR, Rao VK, Mall DM, Gowd TN (2005) Geothermal structure in a seismoactive region of Central India. Pure Appl Geophys 162:129–144
Spector A, Grant FS (1970) Statistical models for interpreting aeromagnetic data. Geophysics 35:293–302
Stüwe K (2007) Geodynamics of the lithosphere: an introduction, 2nd edn. Springer, Berlin, p 493
Tezcan AK (1995) Geothermal explorations and heat flow in Turkey. In: Gupta ML, Yamano M (eds) Terrestrial heat flow and geothermal energy in Asia. Science Publishers, Lebanon, pp 23–42

Tezcan AK, Turgay MI (1989) Heat flow map of Turkey. General Directorate of Mineral Research and Exploration (MTA), Department of Geophysics Research, Ankara (in Turkish, unpublished)
Treitel S, Clement WG, Kaul RK (1971) The spectral determination of depths to buried magnetic basement rocks. Geophys J Roy Astron Soc 24:415–428
Turcotte DL, Schubert G (2002) Geodynamics, 2nd edn. Cambridge University Press, Cambridge
Ustaömer T, Robertson AHF (1995) Palaeotethyan tectonic evolution of the north Tethyan margin in the Central Pontides, N Turkey. In: Erler A, Ercan T (eds) Proceedings of the international symposium on the geology of the Black Sea Region, Ankara, pp 23–42
Ustaömer T, Robertson AHF (1997) Tectonic-sedimentary evolution of the North-Tethyan active margin in the Central Pontides of Northern Turkey. In: Robinson AG (ed) Regional and petroleum geology of the Black Sea Region. AAPG Memoir, vol 68. pp 245–290
Van Der Voo R (1968) Jurassic, Cretaceous and Eocene pole positions from northeastern Turkey. Tectonophysics 6:251–269
Yılmaz Y, Tüysüz O, Yığıtbaş E, Can Genç Ş, Şengör AMC (1997) Geology and tectonic evolution of the Pontides, In: Robinson AG (ed) Regional and petroleum geology of the Black Sea and surrounding region: AAPG Memoir, vol 68, pp 183–226